Viruses that 'infect' viruses: Cas12f1 and Cas9 gene drive in HSV1

Qiaorui Yao[1,*], Zhuangjie Lin[1,*], Keyuan Lai[1,*], Xianyin Zeng[1], Guangxiong Lei[2], Tongwen Zhang[1,†], Hongsheng Dai[1]

1, School of Basic Medicine, Southern Medical University, Guangzhou, China,

2, School of Medicine, College of Southern Hunan, Chenzhou, China.

*, contributed equally

[†], Present affiliation: Vaccine Biotech (Shenzhen) LTD, Shenzhen, China, & Boji Biopharmaceutical, Guangzhou, China

Correspondence: Hongsheng Dai, daihsh@gmail.com

Abstract

Cas9-based synthetic gene drives constitute some minimal elements capable of editing DNA with sequence specificity. However, they face high resistance rate and mitigation strategies developed so far are difficult to implement. Here, we engineered herpes simplex virus type 1 (HSV1) as a vector for gene drive, generated viruses carrying either Cas9 or Cas12f1 gene drives, and compared their performance in spreading the gene drive and causing resistance. Based on phenotypical staining and NGS sequencing, we showed that HSV1 supported fast and effective transmission of gene drive, and Cas12f1 gene drive yielded higher conversion and lower resistance than Cas9 gene drive. Cas12f1 gene drive is a promising alternative to Cas9 gene drive, and HSV1 is a reliable and fast platform to evaluate gene drive. Gene drive viruses worked like pathogens that specifically infect viruses and could potentially be used to attenuate viral infection.

Introduction

Gene drive is a super mendelian inheritance in which particular genetic sequences are passed to the next generation in a biased manner, resulting in the dominant spread of corresponding traits within a target population[1]. Natural gene drives are mainly "selfish genes", such as transposons, homing endonuclease genes, meiotic drive genes, and they have been modified to reduce the survival or reproduction of pests[2]. However, they were not broadly adopted due to low efficiency, poor operationality, and most importantly the inevitable emergence of resistance, which prevents the spread of the drive and its intended effects[3].

CRISPR-Cas is a gene-editing technique that alters DNA sequences with accuracy and effectiveness [4-6]. It involves a Cas nuclease and a short guide RNA (sgRNA). Cas9 is a widely used Cas nuclease and serves as a model for other Cas nucleases. The sgRNA has two components: a 20-nucleotide region that matches the target DNA, and a scaffold that interacts with Cas9. The sgRNA guides the Cas 9 to the specific location in the genome by forming base pairs with the target DNA. Cas 9 is then allosterically activated by the protospacer adjacent motif (PAM), a 2–6 bp sequence immediately following the target DNA sequence, and cut inside the DNA target 3-4 bp upstream of PAM, creating a double-strand break (DSB)[7,8]. The cell then repairs the DSB using non-homologous end joining (NHEJ) or homology directed repair (HDR). NHEJ directly reconnects broken ends of DNA and often introduces small insertion or deletion (indel). HDR is a more accurate process that uses a homologous DNA template to fix the DSB. By providing an exogenous DNA template with desired modifications, CRISPR-Cas can introduce precise changes to the genome through HDR[9].

CRISPR-Cas system has galvanized a new wave of interest in developing CRISPR-based synthetic gene drive as a tool for population control[2]. CRISPR-Cas9 gene drive in general consists of DNA sequences that encode both Cas9 nuclease and sgRNA, and adjacent DNA segments (~1kb in length on each side) that match the locus targeted by sgRNA [10,11]. CRISPR-Cas9 gene drive specifically induces DSBs on the targeted allele and then guides HDR repair by using itself as the template, resulting in the integration and spread of the drive over generations. Gene drive based on CRISPR-Cas9 has been established in yeast[12,13], drosophila[10,11], mosquito[14,15], mouse[16] and lately a human DNA virus[17].

Like other gene drives, CRISPR-Cas9 gene drives could be stopped by resistant alleles. Resistance to gene drive mainly arises from mutations in the target sequence that block the action of CRISPR-Cas9[18,19]. Gene drive resistance has been studied with computational modeling [20,21], or by experimentally tracking gene drive resistance in insects[18,19,22,23]. The relative slow pace of sexual reproduction in insects (i.e., one generation needs 10 days for fly housed at 25°c), however, necessitates a long time for genetic changes to spread and accumulate in a population, making such experiments very time-consuming and difficult to scale up. It would be very helpful to have a new gene drive carrier that could be conveniently manipulated and support fast spread of gene drive.

Cas9 nuclease is a large protein of 1368 amino acids that poses challenges for viral vector delivery[24]. To overcome this limitation, smaller Cas nucleases have been searched for or engineered, resulting in a variety of alternatives [25-31]. One of them is Cas12f1, a 529 amino acids type-V CRISPR nuclease from archaea, which was initially unable to edit double-stranded DNA[32]. However, Cas12f1 achieved efficient and specific genome-editing with a modified guide RNA[25,28,30]. Unlike Cas9, Cas12f1 cleaves dsDNA outside the sgRNA target and PAM, so the target site is likely preserved even after indel mutations by NHEJ[25]. Because of its smaller size and a different DNA cleavage pattern, Cas12f1 may offer some advantages over Cas9. However, Cas12f1-based gene drive has not been reported so far and its performance remains unknown.

HSV1 has a double strand DNA (dsDNA) genome and is amenable to be edited by CRISPR-Cas9 [33,34]. Like many other dsDNA viruses, HSV1 viruses are considered monoploid because each virion contains only one copy of genome. However, HSV1 viruses usually produce many copies of genome that are coexisting in the nucleus before being packaged into new virions, and one host cell could be infected simultaneously by multiple HSV1 virions. These biological features of HSV1 thus create opportunities for genetic materials to be transferred horizontally between viral genomes (Fig 1). HSV1's dsDNA genome (~150kb) has many dispensable regions that potentially could be replaced with gene drive elements[35]. Furthermore, HSV1 infects a broader range of host cells, produces thousands of genome copies in one cell, and finishes an infection/ replication cycle in 12 hours. These features make HSV1 an ideal vector to test gene drive and monitor resistance.

In this study, we created HSV1 viruses that carried either Cas9 or Cas12f1-based gene drive,

evaluated their transmission dynamics, and investigated the difference between Cas9 and Cas12f1 gene drive in generating resistance for the first time. We found that Cas12f1 gene drive rarely produced resistance and that HSV1 gene drive was a powerful tool for evaluating gene drive performance at a fast pace.

Results

Generation of HSV1 gene drive viruses

HSV1 has a linear dsDNA genome, containing 74 open reading frames[35]. The HSV1 genes UL3 and UL4 play no essential role in HSV1 replication, and the UL3-UL4 intergenic region has been reported to be a safe harbor that tolerates the insertion of large DNA fragments without sacrificing HSV1 infectivity and replication[36]. We first validated the tolerability of UL3-UL4 intergenic region by generating virus V19, in which the UL3-UL4 junction was replaced with sequences encoding mCherry (Fig 2A). Recombinant V19 viruses were recovered by transfection of 293T cells with plasmid sgRNA1 and V19 (Supp Sequences) , and infection with HSV1 strain F (wildtype, WT hereafter) (Fig 2B). Single clone of V19 was purified and confirmed by PCR and sequencing (Fig 2D), validating that the UL3-UL4 intergenic region was suitable for engineering.

To make gene drive constructs targeting the UL3-UL4 intergenic region, we modified plasmid V19 by replacing the mCherry expressing cassette with elements that are required to produce sgRNA and express Cas nuclease Cas12f1 or Cas9 (Figure 2A). To help isolate and track gene drive viruses, GFP was linked downstream of the nuclease via the T2A peptide (Fig. 2A). The two Cas12f1 genes drive V23 and V24 produce sgRNAs targeting different sites within the UL3-UL4 intergenic region (Supp. Fig. 1). The two Cas9 genes drive V25 and V28 target the same site, but the expression of Cas9 is driven by CAG or EF1 promoter, respectively. All gene drive viruses were recovered after transfection of 293T cells with individual gene drive plasmid and infection with WT viruses (Fig. 2C). The gene drive plasmids produced Cas nuclease and sgRNA for site-specific cleavage of DNA, and meanwhile served as the template for HDR. After 3-4 rounds of plaque purification using GFP as the selection marker, single clones for each gene drive virus were verified with junctional PCR using primer pairs that bordered the homology arms and amplified only viruses with correct genome (Fig.

2D, Supp Table 1 and 2).

Basic properties of HSV1 gene drive viruses

Virus V19 infected and replicated like WT (Fig. 3A, B), confirming again that the UL3-UL4 junction is suitable for editing. Gene drive viruses V23, V25 and V28 produced plaques with size similar to WT (Fig. 3A, B). The titers of the two Cas9 gene drive viruses, V25 and V28, were slightly lower than that of WT, V19 and V23 (Fig. 3C). V23 and V24 have nearly identical gene drives, however, the single clone of V24 recovered in this study showed smaller plaques and a 10-fold lower titer (Fig. 3A-C). Due to the large size of the HSV1 genome, no attempt was made to identify the cause of this attenuated phenotype or to purify other clones of V24 with more favorable replication. Instead, this V24 clone provided an opportunity to test if lower replication dynamics could affect the spread of gene drive.

After cells were infected with gene drive viruses, GFP expression was observed from the early stage of infection, which reported the production of Cas9 or Cas12f1 and increased in proportion to the expression of HSV1 antigen (Fig. 3D). Although Cas12f1 is about 1/3 the size of Cas9, the extra length of Cas9 seemed have little effect on GFP expression, as the GFP expression levels and kinetics of all gene drive viruses did not show much difference (Fig. 3D).

Gene drive viruses converted WT locus

Multiple HSV1 virions can infect the same host cell and initiate their own replication, providing the opportunity for viruses with different genomes to interact. To test if the gene drive viruses could convert WT locus, we co-infected vero cells with WT (moi=4) and each of the four gene drive viruses (moi=1) (Fig. 4A). The resultant virus-containing supernatant were harvested at 24 hours post infection, diluted to infect BHK cells at moi<0.1 for titrating viruses using fluorescent staining. Expression of HSV1 antigen gD and GFP set apart WT (gD^+, GFP-) and gene drive viruses (gD^+, GFP^+) (Fig. 4B). Although gene drive viruses accounted for ~20% of the input viruses (P0), their proportion in the progeny increased significantly even after one cycle of coinfection (P1), and they become the dominant population after two cycles of coinfection (P2) (Fig. 4C).

Coinfection was also conducted between gene drive viruses (GFP^+, $mCherry^-$) and V19(GFP^-,

mCherry^{+}) (Fig. 4D). The Virus V19 has UL3-UL4 intergenic region replaced with mCherry, and thus has no target for either of the gene drive viruses (Fig. 2A). The percentage of gene drive viruses fluctuated but was within a range close to their starting proportion in the input viruses, and no consistent amplification of GFP^{+} gene drive viruses was observed during co-infection with V19 (Figure 4E ,F). Although the flowcytometry results showed there were few GFP^{+} and mCherry^{+} cells in some samples, we conducted plaque assay using the same supernatants and found no plaque expressing both GFP and mCherry in hundreds of plaques screened (Supp. Fig. 2). Those few double positive dots were likely doublets or rare cells infected by more than two viruses.

Gene drive viruses V23, V24, V25, and V28 replicated at a level close to or even lower than those of WT or V19 (Fig. 3C). The specific expansion of gene drive viruses with WT but not with V19 therefore suggested that transmission of gene drive occurred and required the presence of target sites.

Impact of fitness cost on the spread of gene drive

The fitness costs of gene drives in insects and other higher organisms often hinder the spread of gene drives[37]. Could this also happen with viral gene drives? Although V24, V25, and V28 exhibited a slight fitness loss as indicated by their replication dynamics (Fig. 3 A–C), they efficiently expanded the drive at a rate comparable to V23 (Fig. 4 B, C). To investigate how fitness loss affects the spread of viral gene drive, we created an HSV1 gene drive strain with a known attenuated phenotype. We deleted most of the Us8 gene, which encodes glycoprotein E (gE), from the HSV1 genome. HSV1 gE is not essential for viral replication, but it enhances HSV1 transmission between cells[35,38]. We named the virus V10 (Fig. 5A, Supp. Fig. 3). V10 formed smaller plaques, but produced viral titers similar to WT, indicating a reduced transmission phenotype (Fig. 5B-D). We also made the gene drive virus V15 by replacing the Us8 gene with a cassette expressing sgRNA and Cas9-T2a-GFP (Fig. 5A, Supp. Fig. 3). V15 encodes a Us8-specific sgRNA. The gene drive virus V15 showed the same phenotype as V10 and a slight fitness loss, as evidenced by its smaller plaques compared to WT (Fig. 5B-D). Both V10 and V15 lacked gE expression due to the deletion of Us8 (Fig. 5E).

We next co-infected vero cells with virus V19 (moi=4) and V15 (moi=1) (Fig. 5F), collected progeny virus 24 hours after each passage, and quantified viruses by fluorescent staining (Fig. 5G). Gene drive transfer from V15 to V19 yielded new gene drive viruses expressing both GFP and mCherry

(Figure 5G-I). Gene drive viruses, including GFP^+ $mCherry^-$ and GFP^+ $mCherry^+$ populations, comprised 90% of all viruses after two passages (Fig. 5H), an efficiency not inferior to gene drive viruses with WT phenotype (Fig 4 B-C). From the cases we evaluated in this study, a mild fitness loss seemed not impair the transmission of gene drive significantly.

Transmission dynamics of Cas12f1 and Cas9 gene drives

V23, V24, V25, and V28 viruses all carried functional gene drives and successfully invaded WT viruses, however the resulting gene drive viruses were identical to the input gene drive viruses (Fig. 4A, B). To compare the transmission dynamics of Cas12f1 and Cas9 gene drives, we used V10 virus as the recipient of gene drive (Fig. 6A). The resultant new gene drive viruses were gD^+ GFP^+ gE^-, readily distinguishable from the input gene drive viruses V23, V24, V25, and V28, which were gD^+ GFP^+ gE^+ (Fig. 6A, B, Supp Fig 4-7).

At the initial ratio of 4:1 (total moi=5, V10 : gene drive=4:1), all four gene drive viruses steadily converted V10 viruses, and those newly converted gene drive viruses became dominant after 4 passages and eventually competed out input gene drive viruses (Fig. 6C). The two Cas12f1 gene drives (V23 and V24) spread similarly fast as the two Cas9 gene drives (V25 and V28). However, gene drive viruses V25 and V28 encountered resistance after P5, and some residual V10 even bounced back slightly after more passages.

We also tested coinfection of vero cells with more V10 (moi=4.75) and gene drive virus (moi=0.25). Based on Poisson distribution, the chance that a cell is coinfected by V10 and at least one gene drive virion is 22%. At this lower initial ratio, the Cas12f1 gene drive V23 and V24 spread much slower, and converted almost all input viruses until P11. The lower initial frequency of Cas9 gene drive V25 and V28, however, only slowed gene drive propagation in the first 3 passages, spread of Cas9 gene drive picked up at P4 and quickly reached equilibrium with V10 at P5.

Therefore, cas12f1 gene drive and Cas9 gene drive differed greatly in two aspects. First, the Cas9 gene drives spread faster than Cas12f1 gene drives. Second, the Cas12f1 gene drive converted almost all of the input V10 virus to gene drive viruses, whereas the Cas9 gene drive failed to convert a large portion of V10 viruses, which may contain clones resistant to Cas9-gRNA (Fig. 6D). The two Cas12f1 gene drive behaved the same at either of the ratio, and so did the two Cas9 gene drives.

Resistance profile of Cas9 and Cas12f1 gene drives

DSBs caused by gene drives can be repaired by error-prone NHEJ, which may modify the sgRNA target site and confer resistance to gene drives. To investigate how gene drive transmission could remodel the V10 genome and generates variants that are resistant to gene drives, we collected viruses at P0 (input virus), P1, P4, and P7, amplified the short UL3-UL4 intergenic sequences (Supp. Fig 1), and conducted NGS amplicon sequencing (Fig 7A). Due to the short PCR extension time (20 s), gene drive viruses could not be amplified, but the primers may also anneal to gene drive sequences, resulting in false priming or primer-dimers.

In P1, V10 viruses were prevalent, gene drive viruses did not interfere with PCR, and most NGS reads (>98%) mapped to the reference UL3-UL4 intergenic sequence with intact sgRNA target sites (Fig. 7B). The diversity of P1 was similar to that of P0. In P4 and P7, gene drive viruses were dominant, causing more interference on PCR, and an increasing number of NGS reads failed to map to the reference (Fig. 7B). In P4 and P7, the vast majority of V10 viruses had been converted to gene drives, but the remaining unconverted V10 viruses were not unchanged. Co-infection with gene drive viruses produced V10 viruses with mutated sgRNA targets. Cas12f1 gene drives and Ca9 gene drives however reshaped the V10 viruses differently (Fig. 7B). In V10:V23 or V10:V24 coinfections, 90.9% (V10:V23) or 82.6% (V10:V24) of all mapped reads still had intact sgRNA targets even after 7 passages. On the other hand, V25 and V28 gene drives progressively generated V10 variants with mutations in the sgRNA target, and only 5.5% (V10:V25) or 11.9% (V10:V28) of mapped reads remained unchanged in P7.

We analyzed the mutations in all the mapped reads and acquired the cumulative mutation rate for each base of the UL3-UL4 intergenic region. Mutations can happen naturally during genome replication, or can result from error-prone NHEJ repair of a DSB. NHEJ often generates a high frequency of short indels at DSB junctions. Unexpectedly, we detected few indels in V10 viruses from the three V10:V23 and three V10:V24 coinfection pools (Fig. 7C, D). However, we observed that point mutations were enriched within the Cas12f1 sgRNA target in P4 and P7. Mutation G109A was located on the V23 sgRNA target, and its frequency in mapped reads (0.3% of P1, 0.47 of P4, and 8.3% of P7) increased as V10:V23 coinfection progressed (Fig. 7C, Supp. Fig. 1). Mutations

G83A and T92G, which disrupted the V24 sgRNA target, were the two main mutations accumulated in V10:V24 coinfections (Fig. 7D, Supp. Fig. 1).

The V25 and V28 gene drives left distinct marks on the remaining V10 genome (Fig. 7E, F). These genetic changes were mostly short indels and centered on the third nucleotide upstream of the PAM. We also observed frequent large deletions (loss >50nt) in 3-7% of the reads in the P4 and P7 pools. However, the two sides of the DSB caused by Cas9 were not affected equally. The 5' side of the breakpoint was truncated more frequently than the 3' side, and there were almost no reads with large deletions across both sides of the breakpoint (Fig. 7G, H). This pattern of variation emerged in P4 and became more pronounced in P7.

Discussion

In this proof-of-concept study, we showed HSV1 viruses could act as gene drive vectors, allowing both Cas9 and Cas12f1 gene drives to invade into viruses with WT alleles. Taking advantage of the fast replication rate of HSV1, spread of gene drive reached plateau in one week, a speed not achieved by any other organisms tested so far [13,16,17,39]. Cas12f1 gene drives effectively converted almost all viruses and rarely produced resistant variants. Cas9 gene drive, however, quickly encountered high percentage (up to 25%) of resistance due to mutations on the target sites.

Several methods have been tested to overcome resistance to Cas9 gene drive in other organisms, such as targeting multiple regions that are conserved or essential for the organism[20,21,40]. Implementing these approaches however is cumbersome and not necessarily effective. Another option is to explore Cas nuclease that would mechanistically induce less mutation to the target site after DSB repair. Cas12a is the only other Cas nuclease implemented for gene drive so far, and have been shown to propagate efficiently in yeast and fruit flies[41 39]. However, Cas12a cut DNA within the sgRNA target sequence [42] and is very sensitive to mismatches between sgRNA and the target DNA[43]. In line with these properties of Cas12a, Víctor López Del Amo et al reported that Cas12a gene drive produced resistant alleles in 5-8% of the target population[39].

We use the improved Cas12f1[25] for gene drive. Cas12f1 cuts the target DNA at 22 and 24 nt upstream of the PAM [44], which intrinsically preserves the sgRNA target sites intact and allows

repeated editing at the same location[25,45]. In editing genome of 293T cells, Cas12f1 showed lower editing efficacy and caused less mutation than Cas9, and the resultant mutations were mainly deletions near the target[25,45]. In consistent with these documented properties of Cas12f1 and Cas9, we observed that the two Cas12f1 gene drives spread a bit slower than the two Cas9 gene drives, but they were all very effective.

However, we found Cas12f1 and Cas9 viral gene drives exhibited some distinct properties. First, the two independent Cas12f1 gene drive viruses, V23 and V24, hardly caused any deletional mutation to the target sites. It is unlikely that we failed to detect indels from the Cas12f1 gene drive pool, because our amplicon NGS sequencing protocol reliably detected a wide range of indels caused by Cas9 gene drives. Cas9 produces blunt-ended DSBs, while Cas12f1 cuts dsDNA to create sticky ends [44], which facilitate HDR when a suitable repair template is present[46]. 293T cells have two copies of each chromosome, but HSV1 viruses are essentially multiploid when they replicate inside cells. Thousands of HSV1 genome copies (both wt. and gene drive) in one cell provided abundant templates for the DSBs to be repaired by HDR. Therefore, we suggested that the sticky ends generated by Cas12f1 and the availability of ample repair templates contributed to the nearly 100% conversion rate of Cas12f1 gene drives in HSV1. It would be worthwhile to investigate if Cas12f1 gene drive could achieve such a high conversion rate in other organisms.

Second, some of the viruses that were not converted by the Cas9 gene drive V25 and V28 had large deletions in their genomes, mostly on the 5' side of the site where Cas9 cut. Directional editing is a property of some CRISPR nucleases, for example, Cas3 induced large deletions predominantly upstream of PAM[47]. However, this has not been reported for Cas9 before. Since V25 and V28 targeted the same sequences, we cannot rule out that this deletion pattern is specific to this target. However, our findings raise an interesting question: are the two ends of the DSB created by Cas9 equal? This could be investigated further by using Cas9 viral gene drives to target different regions of the HSV1 genome or other viruses.

Third, fitness cost could reduce the spread of a gene drive in insects and other higher organisms[18], but HSV1 gene drives were not very sensitive to fitness loss. Gene drive viruses V24, V25, V28 and V15 all showed certain level of attenuation, but were still highly transmissible. HSV1 viruses

reproduce thousands copies in host cells, as we mentioned before. The coexisting wild type viruses may compensate the defects of the gene drive viruses and possibly explain the high propagation rate of HSV1 gene drive. However, we only tested very limited cases of mild fitness loss, it is yet to define the impact of higher fitness cost on the spread of HSV1 gene drive.

Cas9-based gene drive has been reported for HCMV[17]. Although both HCMV and HSV1 are herpesviruses, they are quite different. HSV1 replicates much faster and at higher titer than HCMV[48]. We initially suspected the short replication cycle of HSV1 might pose challenge for the transmission of gene drive, as it might be too short to complete a multi-step process involving production of sgRNA and Cas nuclease, cleavage of target, and DSB repair by HDR. It turned out both Cas9 and Cas12f1 gene drive spread very efficiently among HSV1 viruses, suggesting that such viral gene drive would work for other herpesviruses as well.

Overall, our study presented the first Cas12f1-based gene drive and established HSV1 as a great tool to study horizontal gene transfer. Cas12f1 gene drive demonstrated high efficiency and low resistance, and could have great potential in controlling pathogens and pests. HSV1 is a safe and versatile vector, as engineered HSV1 viruses have been approved for treating cancer[49] and genetic disease[50]. Our study opens new possibilities for using HSV1 gene drive for prevention and treatment of diseases.

MATERIALS AND METHODS

Cells and viruses: HEK 293T, BHK-21, Vero cells and HSV-1 F strain were obtained from American Type Culture Collection (ATCC). All cells were cultured in DMEM supplemented with 10% fetal bovine serum (FSP500, ExCell Bio) and 10000U/ml penicillin/ streptomycin (BL505A, Biosharp), and maintained at 37□ with 5 % CO2.

Construction of gene drive cassettes: sgRNA targets were picked using the online tool CRISPOR (http://crispor.tefor.net/) and all plasmids were designed using SnapGene® software (Dotmatics; available at snapgene.com). Cas9 was amplified from px330 (Addgene) and Cas12f1 was derived from the optimized Un1Cas12f1 sequence[25] and synthesized (General Biol). Vector backbone and insert fragments was amplified with Q5 high fidelity DNA polymerase (M0491L, NEB), and ligated together with ClonExpress® Ultra One Step Cloning Kit (C112-02, Vyzame). Ligation products were transformed with DH10B competent bacteria, and later single clones were picked and validated by sanger sequencing (Tsingke). Sequences and annotations for all plasmids used in this study were provided in supplemental sequences.

Generation of HSV1 gene drive virus: 293T cells were first transfected with gene drive plasmids that were pre-complexed with PEI (408727-100ML, Sigma-Aldrich), cultured for 12 hours, and then infected with HSV-1 F strain (moi =0.1). Recombination between plasmids and viruses was allowed to continue for 48h, then virus-containing supernatants were harvested. To isolate recombinant viruses, single layer of vero cells were infected with sequentially diluted supernatant for 1 hour, and overlayed with 1% methylcellulose (C6333-250g，Macklin) solubilized in DMEM. Individual plaques expressing reporter gene were picked at 48 hours, and were propagated and purified by additional 3 to 4 rounds of plaque assay. Genome DNA of individual clones was extracted with DNA extraction kit (DC102, Vazyme), amplified with primers (Supplemental Table 1), and validated by sanger sequencing (Tsingke).

Titration of Viruses: It was conducted as described [35], briefly, $2x10^4$ Vero cells were incubated with sequentially diluted viruses at 37□ for 4 hours. Human gamma globulin, which contains polyclonal antibodies against HSV1, was supplemented into the culture to the final concentration of 0.5% (v/v). 48 hours later, plaques were counted under an inverted microscope.

Imaging: Pictures of viral plaques were taken at 48 hours post infection with a Nikon Eclipse Ts2-FL inverted microscope. To compare the plaque size of different viruses, 20 plaques for each virus were randomly picked and the area of each plaque was calculated using Nikon acquisition software NIS-Elements BR 5.30.0364.

Purification of viruses: To prepare virus stocks, BHK-21 or vero cells were infected with HSV1 F strain or its derivatives at moi=0.1. Both cells and supernatant were harvested when cytopathic effect was observed in all cells. Cells were subjected to three freeze-thaw cycles to release viruses. Cell debris was removed by centrifuging at 6000g for 20 minutes. Cleared supernatant was layered on 30%

sucrose and further purified by centrifuge at 12000g for 2 hours. Viruses were aliquoted, titrated, and stored at -80□ until use.

Growth kinetics of viruses: Vero cells seeded in 24-well plates were infected with viruses (moi = 0.1) for 1 hour at room temperature. After washing with PBS, the cells were further cultured in DMEM supplemented with 5% FBS. Supernatants were collected at 12, 24, 36, 48, 60 and 72 hours after infection. Virus titers were determined by the plaque assay.

Transmission of gene drive: Vero cells were initially infected with target viruses and gene drive viruses (total moi=5, target : gene drive=4:1) for 24 hours. According to the Poisson distribution Such a coinfection condition meant that a host cell had 63% probability of being simultaneously infected by WT and at least one gene drive virion. In some cases, additional coinfection with target : gene drive=19:1 was also conducted. Progeny viruses were harvested and passaged to fresh vero cells for new cycles of coinfection as needed. To quantify the composition of viruses, supernatants harvested from each passage were diluted and used to infect fresh BHK cells at low moi (~0.1) for 12 hours, the infected cells were stained with monoclonal antibody against HSV1 gD (sc-21719, Santa Cruz) or gE (sc-69803, Santa Cruz) and a matching fluorescent secondary antibody (A0473, Beyotime). Samples were collected with flowcytometry (NovoCyte, Agilent). The flow cytometry results were analyzed using FlowJo™ v10.8 Software (BD Life Sciences)

NGS Amplicon sequencing and analysis: PCR fragments were amplified by specific primers with adaptors, and sequenced with read length of 150nt from both sides with Illumina Miseq PE150 platform (Tsingke). The paired-end sequencing raw data were first checked by FastQC v0.11.9 (https://www.bioinformatics.babraham.ac.uk /projects/ fastqc/) for quality and then analyzed with commercial software Geneoious Prime 2023.2.1 (https://www. geneious.com). Reference sequences were provided in Supp. Fig. 1. Data were trimmed and mapped to the reference sequences, and neighbor-joining tree for all mapped reads were built using the Tamura-Nei model. Mutation rate at each nucleotide of reference sequences were derived from the phylogenic tree. Indels were defined as small indels (<50□bp) or large indels (50≥□bp).

Statistics and reproducibility

Percentage, mean, CI and standard deviations were calculated using GraphPad Prism 9.5. Sample size was not predetermined, and no data were excluded from the analyses. The experiments were not randomized and the Investigators were not blinded to allocation during experiments and outcome assessment.

Data availability

The amplicon sequencing data have been deposited in the NCBI Gene Expression Omnibus (GEO) database under accession number (will update once manuscript accepted). Request for reagents will be fulfilled by the corresponding author H.D (daihsh@gmail.com) after receiving appropriate MTA.

Acknowledgements

We would like to thank Michael Caligiuri (City of Hope, USA) for his support and guidance. This study was supported by the startup fund from Southern Medical University, and Natural Science Foundation of Guandong Province (2022A1515010421). H.D is a Pearl River Young Scholar.

Contributions

H.D and T.Z conceived and designed the study; Q.Y, Z.L and K.L performed the experiments with the help of X.Z; G.L provided critical reagents; H.D and T.Z analyzed the data and wrote the manuscript.

Competing interests

The authors declare no competing interests.

References

1 Burt, A. Site-specific selfish genes as tools for the control and genetic engineering of natural populations. *Proc Biol Sci* **270**, 921-928, doi:10.1098/rspb.2002.2319 (2003).

2 Bier, E. Gene drives gaining speed. *Nat Rev Genet* **23**, 5-22, doi:10.1038/s41576-021-00386-0 (2022).

3 Price, T. A. R. *et al.* Resistance to natural and synthetic gene drive systems. *J Evol Biol* **33**, 1345-1360, doi:10.1111/jeb.13693 (2020).

4 Cong, L. *et al.* Multiplex genome engineering using CRISPR/Cas systems. *Science* **339**, 819-823, doi:10.1126/science.1231143 (2013).

5 Gasiunas, G., Barrangou, R., Horvath, P. & Siksnys, V. Cas9-crRNA ribonucleoprotein complex mediates specific DNA cleavage for adaptive immunity in bacteria. *Proc Natl Acad Sci U S A* **109**, E2579-2586, doi:10.1073/pnas.1208507109 (2012).

6 Jinek, M. *et al.* A programmable dual-RNA-guided DNA endonuclease in adaptive bacterial immunity. *Science* **337**, 816-821, doi:10.1126/science.1225829 (2012).

384 7 Jinek, M. *et al.* Structures of Cas9 endonucleases reveal RNA-mediated conformational activation.
385 *Science* **343**, 1247997, doi:10.1126/science.1247997 (2014).
386 8 Sternberg, S. H., Redding, S., Jinek, M., Greene, E. C. & Doudna, J. A. DNA interrogation by the
387 CRISPR RNA-guided endonuclease Cas9. *Nature* **507**, 62-67, doi:10.1038/nature13011 (2014).
388 9 Ran, F. A. *et al.* Double nicking by RNA-guided CRISPR Cas9 for enhanced genome editing
389 specificity. *Cell* **154**, 1380-1389, doi:10.1016/j.cell.2013.08.021 (2013).
390 10 Gantz, V. M. & Bier, E. Genome editing. The mutagenic chain reaction: a method for converting
391 heterozygous to homozygous mutations. *Science* **348**, 442-444, doi:10.1126/science.aaa5945
392 (2015).
393 11 Gantz, V. M. *et al.* Highly efficient Cas9-mediated gene drive for population modification of the malaria
394 vector mosquito Anopheles stephensi. *Proc Natl Acad Sci U S A* **112**, E6736-6743,
395 doi:10.1073/pnas.1521077112 (2015).
396 12 DiCarlo, J. E., Chavez, A., Dietz, S. L., Esvelt, K. M. & Church, G. M. Safeguarding CRISPR-Cas9
397 gene drives in yeast. *Nat Biotechnol* **33**, 1250-1255, doi:10.1038/nbt.3412 (2015).
398 13 Xu, H. *et al.* Chromosome drives via CRISPR-Cas9 in yeast. *Nat Commun* **11**, 4344,
399 doi:10.1038/s41467-020-18222-0 (2020).
400 14 Hammond, A. *et al.* A CRISPR-Cas9 gene drive system targeting female reproduction in the malaria
401 mosquito vector Anopheles gambiae. *Nat Biotechnol* **34**, 78-83, doi:10.1038/nbt.3439 (2016).
402 15 Kyrou, K. *et al.* A CRISPR-Cas9 gene drive targeting doublesex causes complete population
403 suppression in caged Anopheles gambiae mosquitoes. *Nat Biotechnol* **36**, 1062-1066,
404 doi:10.1038/nbt.4245 (2018).
405 16 Grunwald, H. A. *et al.* Super-Mendelian inheritance mediated by CRISPR-Cas9 in the female mouse

406 germline. *Nature* **566**, 105-109, doi:10.1038/s41586-019-0875-2 (2019).

407 17 Walter, M. & Verdin, E. Viral gene drive in herpesviruses. *Nat Commun* **11**, 4884,

408 doi:10.1038/s41467-020-18678-0 (2020).

409 18 Drury, D. W., Dapper, A. L., Siniard, D. J., Zentner, G. E. & Wade, M. J. CRISPR/Cas9 gene drives in

410 genetically variable and nonrandomly mating wild populations. *Sci Adv* **3**, e1601910,

411 doi:10.1126/sciadv.1601910 (2017).

412 19 Hammond, A. M. *et al.* The creation and selection of mutations resistant to a gene drive over multiple

413 generations in the malaria mosquito. *PLoS Genet* **13**, e1007039, doi:10.1371/journal.pgen.1007039

414 (2017).

415 20 Noble, C., Olejarz, J., Esvelt, K. M., Church, G. M. & Nowak, M. A. Evolutionary dynamics of CRISPR

416 gene drives. *Sci Adv* **3**, e1601964, doi:10.1126/sciadv.1601964 (2017).

417 21 Champer, S. E. *et al.* Computational and experimental performance of CRISPR homing gene drive

418 strategies with multiplexed gRNAs. *Sci Adv* **6**, eaaz0525, doi:10.1126/sciadv.aaz0525 (2020).

419 22 Fuchs, S. *et al.* Resistance to a CRISPR-based gene drive at an evolutionarily conserved site is

420 revealed by mimicking genotype fixation. *PLoS Genet* **17**, e1009740,

421 doi:10.1371/journal.pgen.1009740 (2021).

422 23 Champer, J. *et al.* Novel CRISPR/Cas9 gene drive constructs reveal insights into mechanisms of

423 resistance allele formation and drive efficiency in genetically diverse populations. *PLoS Genet* **13**,

424 e1006796, doi:10.1371/journal.pgen.1006796 (2017).

425 24 Hsu, P. D., Lander, E. S. & Zhang, F. Development and applications of CRISPR-Cas9 for genome

426 engineering. *Cell* **157**, 1262-1278, doi:10.1016/j.cell.2014.05.010 (2014).

427 25 Kim, D. Y. *et al.* Efficient CRISPR editing with a hypercompact Cas12f1 and engineered guide RNAs

428 delivered by adeno-associated virus. *Nat Biotechnol* **40**, 94-102, doi:10.1038/s41587-021-01009-z
429 （2022）.
430 26 Schmidt, M. J. *et al.* Improved CRISPR genome editing using small highly active and specific
431 engineered RNA-guided nucleases. *Nat Commun* **12**, 4219, doi:10.1038/s41467-021-24454-5
432 （2021）.
433 27 Bigelyte, G. *et al.* Miniature type V-F CRISPR-Cas nucleases enable targeted DNA modification in
434 cells. *Nat Commun* **12**, 6191, doi:10.1038/s41467-021-26469-4（2021）.
435 28 Xu, X. *et al.* Engineered miniature CRISPR-Cas system for mammalian genome regulation and
436 editing. *Mol Cell* **81**, 4333-4345 e4334, doi:10.1016/j.molcel.2021.08.008（2021）.
437 29 Wang, Y. *et al.* A highly specific CRISPR-Cas12j nuclease enables allele-specific genome editing. *Sci*
438 *Adv* **9**, eabo6405, doi:10.1126/sciadv.abo6405（2023）.
439 30 Wu, Z. *et al.* Programmed genome editing by a miniature CRISPR-Cas12f nuclease. *Nat Chem Biol*
440 **17**, 1132-1138, doi:10.1038/s41589-021-00868-6（2021）.
441 31 Kong, X. *et al.* Engineered CRISPR-OsCas12f1 and RhCas12f1 with robust activities and expanded
442 target range for genome editing. *Nat Commun* **14**, 2046, doi:10.1038/s41467-023-37829-7（2023）.
443 32 Harrington, L. B. *et al.* Programmed DNA destruction by miniature CRISPR-Cas14 enzymes. *Science*
444 **362**, 839-842, doi:10.1126/science.aav4294（2018）.
445 33 Suenaga, T., Kohyama, M., Hirayasu, K. & Arase, H. Engineering large viral DNA genomes using the
446 CRISPR-Cas9 system. *Microbiol Immunol* **58**, 513-522, doi:10.1111/1348-0421.12180（2014）.
447 34 Bi, Y. *et al.* High-efficiency targeted editing of large viral genomes by RNA-guided nucleases. *PLoS*
448 *Pathog* **10**, e1004090, doi:10.1371/journal.ppat.1004090（2014）.
449 35 Dai, H. S. *et al.* The Fc Domain of Immunoglobulin Is Sufficient to Bridge NK Cells with Virally Infected

450 Cells. *Immunity* **47**, 159-170 e110, doi:10.1016/j.immuni.2017.06.019 (2017).

451 36 Morimoto, T., Arii, J., Akashi, H. & Kawaguchi, Y. Identification of multiple sites suitable for insertion of
452 foreign genes in herpes simplex virus genomes. *Microbiol Immunol* **53**, 155-161, doi:10.1111/j.1348-
453 0421.2008.00104.x (2009).

454 37 Hammond, A. *et al.* Regulating the expression of gene drives is key to increasing their invasive
455 potential and the mitigation of resistance. *PLoS Genet* **17**, e1009321,
456 doi:10.1371/journal.pgen.1009321 (2021).

457 38 Wisner, T., Brunetti, C., Dingwell, K. & Johnson, D. C. The extracellular domain of herpes simplex
458 virus gE is sufficient for accumulation at cell junctions but not for cell-to-cell spread. *J Virol* **74**, 2278-
459 2287, doi:10.1128/jvi.74.5.2278-2287.2000 (2000).

460 39 Sanz Juste, S., Okamoto, E. M., Nguyen, C., Feng, X. & Lopez Del Amo, V. Next-generation CRISPR
461 gene-drive systems using Cas12a nuclease. *Nat Commun* **14**, 6388, doi:10.1038/s41467-023-42183-
462 9 (2023).

463 40 Bishop, A. L. *et al.* Double-tap gene drive uses iterative genome targeting to help overcome
464 resistance alleles. *Nat Commun* **13**, 2595, doi:10.1038/s41467-022-29868-3 (2022).

465 41 Lewis, I. C., Yan, Y. & Finnigan, G. C. Analysis of a Cas12a-based gene-drive system in budding
466 yeast. *Access Microbiol* **3**, 000301, doi:10.1099/acmi.0.000301 (2021).

467 42 Stella, S., Alcon, P. & Montoya, G. Structure of the Cpf1 endonuclease R-loop complex after target
468 DNA cleavage. *Nature* **546**, 559-563, doi:10.1038/nature22398 (2017).

469 43 Kim, D. *et al.* Genome-wide analysis reveals specificities of Cpf1 endonucleases in human cells. *Nat*
470 *Biotechnol* **34**, 863-868, doi:10.1038/nbt.3609 (2016).

471 44 Takeda, S. N. *et al.* Structure of the miniature type V-F CRISPR-Cas effector enzyme. *Mol Cell* **81**,

472 558-570 e553, doi:10.1016/j.molcel.2020.11.035（2021）.

473 45 Xin, C. *et al.* Comprehensive assessment of miniature CRISPR-Cas12f nucleases for gene disruption.

474 *Nat Commun* **13**, 5623, doi:10.1038/s41467-022-33346-1（2022）.

475 46 Zhao, Z., Shang, P., Sage, F. & Geijsen, N. Ligation-assisted homologous recombination enables

476 precise genome editing by deploying both MMEJ and HDR. *Nucleic Acids Res* **50**, e62,

477 doi:10.1093/nar/gkac118（2022）.

478 47 Morisaka, H. *et al.* CRISPR-Cas3 induces broad and unidirectional genome editing in human cells.

479 *Nat Commun* **10**, 5302, doi:10.1038/s41467-019-13226-x（2019）.

480 48 Vastag, L., Koyuncu, E., Grady, S. L., Shenk, T. E. & Rabinowitz, J. D. Divergent effects of human

481 cytomegalovirus and herpes simplex virus-1 on cellular metabolism. *PLoS Pathog* **7**, e1002124,

482 doi:10.1371/journal.ppat.1002124（2011）.

483 49 Zhang, T. *et al.* Talimogene Laherparepvec（T-VEC）: A Review of the Recent Advances in Cancer

484 Therapy. *J Clin Med* **12**, doi:10.3390/jcm12031098（2023）.

485 50 Gurevich, I. *et al.* In vivo topical gene therapy for recessive dystrophic epidermolysis bullosa: a phase

486 1 and 2 trial. *Nat Med* **28**, 780-788, doi:10.1038/s41591-022-01737-y（2022）.

487

488

Figure Legend

Fig.1. Schematic depiction of HSV1 gene drive. CRISPR-based gene drive is composed of Cas nuclease and sgRNA. In this study, both Cas9 and Cas12f1 gene drives were generated. When wt HSV1 viruses and gene drive viruses co-infect one cell, sgRNA and Cas nuclease produced by gene drive viruses cut dsDNA viral genome at the sgRNA target locus and causes DSBs. DSBs could be repaired by HDR using the genome of gene drive viruses as the template, converting wt to gene drive viruses. If DSBs were repaired by NHEJ, mutations might be introduced to eliminate the sgRNA targets, leading to resistant variants to the gene drive. Uncut genome would be packaged to form wt viruses and unrepaired DSBs be lost.

Fig.2. Generation of gene drive viruses. A, schematic genetic organization of plasmids and the resultant recombinant HSV1 viruses. B. generation of recombined V19 virus using Cas9-assisted HDR with two separate plasmids. Plasmid sgRNA1 encodes Cas9 and sgRNA targeting UL3-UL4 intergenic region, plasmid V19 played as the template for HDR. B, gene drive viruses, including V23, V24, V25 and V28, were generated by transfection of gene drive plasmids and infection of WT viruses. C. Agarose gel showing junctional PCR fragments of recombinant HSV1 viruses. Genomic DNA from single clones of each virus were amplified with primer pairs listed in Supp Table 1 and 2.

Fig.3. Basic properties of gene drive viruses. A, appearance of a typical plaque of HSV1 viruses on vero cells at 48h post infection. Scale bar, 200uM. B, plaque sizes of HSV1 viruses on vero cells at 48 hours post infection. 20 plaques from each virus were randomly picked and the area for each plaque was calculated and plotted, mean with 95% CI was marked for each viruses. * $P<0.05$. C, one step growth curve of HSV1 viruses. D, expression of GFP and HSV1 antigens at different time points after BHK cells were infected with HSV1 viruses.

Fig.4. HSV1 gene drive viruses propagated with wildtype viruses, but not with viruses lack of sgRNA target. A, schematic diagram showing the process and consequence of the spread of gene drive viruses with wildtype viruses. Progeny viruses could be passaged for more rounds to convert all wt locus. B and C, the composition of gene drive virus (GFP^+, gD^+) and wt virus (GFP^-, gD^+) before (P0) and after each passage (P1, P2). BHK cells were infected with diluted virus-containing supernatant for 12 hours, and labeled with antibody. Representative (B) and statistic summary (C) of

3 experiments were shown. D, schematic diagram showing the process and consequence of the spread of gene drive viruses with V19. E and F, the composition of gene drive virus (GFP^+) and V19 ($mCherry^+$) before (P0) and after each passage (P1, P2). BHK cells were infected with diluted virus-containing supernatant for 12 hours, and measure for the expression of GFP and mCherry. Representative (E) and statistic summary (F) of 3 experiments were shown. * $p<0.05$ by comparing with P0.

Fig.5. HSV1 gene drive viruses with decreased fitness could spread efficiently. A, schematic genome organization of wt HSV1 and engineered HSV1 viruses with modification at the Us8 locus. B, appearance of a typical plaque of HSV1 viruses on vero cells at 48 hours post infection. Scale bar, 200uM. C, plaque sizes of HSV1 viruses on vero cells at 48 hours post infection. 20 plaques from each virus were randomly picked and the area for each plaque was calculated and plotted, mean with 95% CI was marked for each strain. * $P<0.05$. D, one step growth curve of HSV1 viruses. E, expression of GFP and HSV1 antigens at 12 hours after BHK cells were infected with HSV1 viruses (MOI=2). F, schematic diagram showing the process and consequence of the spread of V15 gene drive viruses with V19. Progeny viruses could be passaged for more rounds to let V15 convert most Us8 locus in V19 viruses. G-I, the composition of V15 (GFP^+) , V19 ($mCherry^+$) and the newly converted gene drive virus (GFP^+ & $mCherry^+$) before (P0) and after each passage (P1, P2, P3). In the two independent experiments, vero cells were initially infected with different total amount of viruses (but V15:V19 were close to 1:4 in both cases), virus-containing supernatant at each passage were titrated by infecting BHK cells for 12 hours and measuring the percentage of GFP^+ and/or $mCherry^+$ (G), and the relative ratio of each strain was calculated (H). I, P1 supernatant was diluted and plaqued on vero cells for 48h. Plaques were imaged for the expression of fluorescent proteins. Scale bar, 500uM.

Fig.6. Transmission dynamics of HSV1 gene drive viruses and rise of resistant clones. A, schematic diagram showing the process and possible consequence of the spread of gene drive viruses with V10. V10 (gD^+ gE^-) could be converted by original gene drive viruses (gD^+ GFP^+ gE^+) or by newly-generated gene drive viruses (gD^+ GFP^+gE^-). After each coinfection, progeny viruses were passaged to fresh vero cells for a new cycle of coinfection. B-D, quantification of V10, original gene drive

viruses and the newly-converted gene drive virus after each passage by fluorescent staining. B, staining results for V10 and V23 coinfection at initial ratio of 4:1. C and D, summary of the relative ratio of each strain after each passage with initial ratio of V10: gene drive= 4:1 or 19:1. Blue bar, green bar and yellow bar represents V10, input gene drive and the newly-converted gene drive viruses, respectively. D, plot of the percentage of newly-converted gene drive viruses at each passage.

Fig.7. Target sites sequencing uncovered difference between Cas12f1 and Cas9 gene drive. A, diagram showing PCR and sequencing procedures. Input viruses (P0), P1, P4 and P7 supernatants from coinfection with initial ratio of V10: gene drive=4:1 were amplified and sequenced. B, total amplicon reads for each sample and distribution of reads that were mapped or not to the reference. C-F. distribution and frequency of mutations along the reference sequences for V10:V23 (C), V10:V24 (D), V10:V25 (E) and V10:V28 (F). The localization of sgRNA target sequences and PAM were marked with blue-red bar. G and H, non-redundant indels from P7 of V10:V25 (G) or V10:V28 (H) were mapped to the reference sequences. Each bar represents a unique read, breaks linked by dashed lines are deletions, sporadic blue marks represent point mutations.

Fig 1

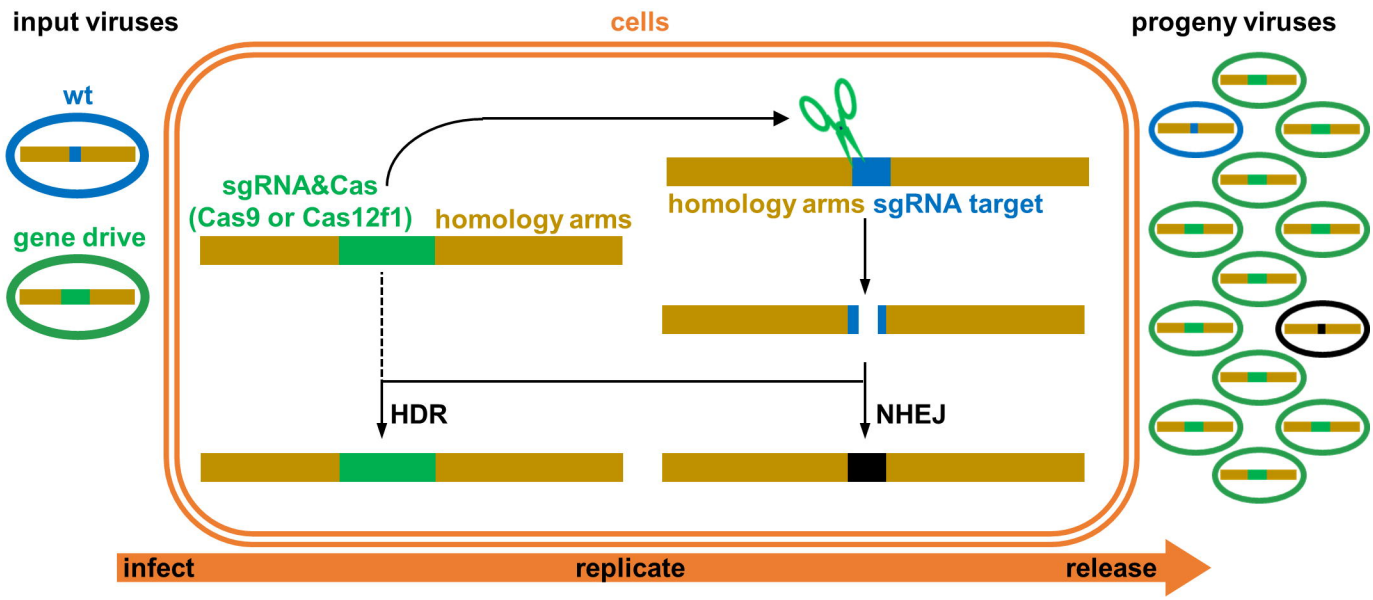
input viruses
cells
progeny viruses
wt
gene drive
sgRNA&Cas
(Cas9 or Cas12f1)
homology arms
homology arms
sgRNA target
HDR
NHEJ
infect
replicate
release

Fig 2

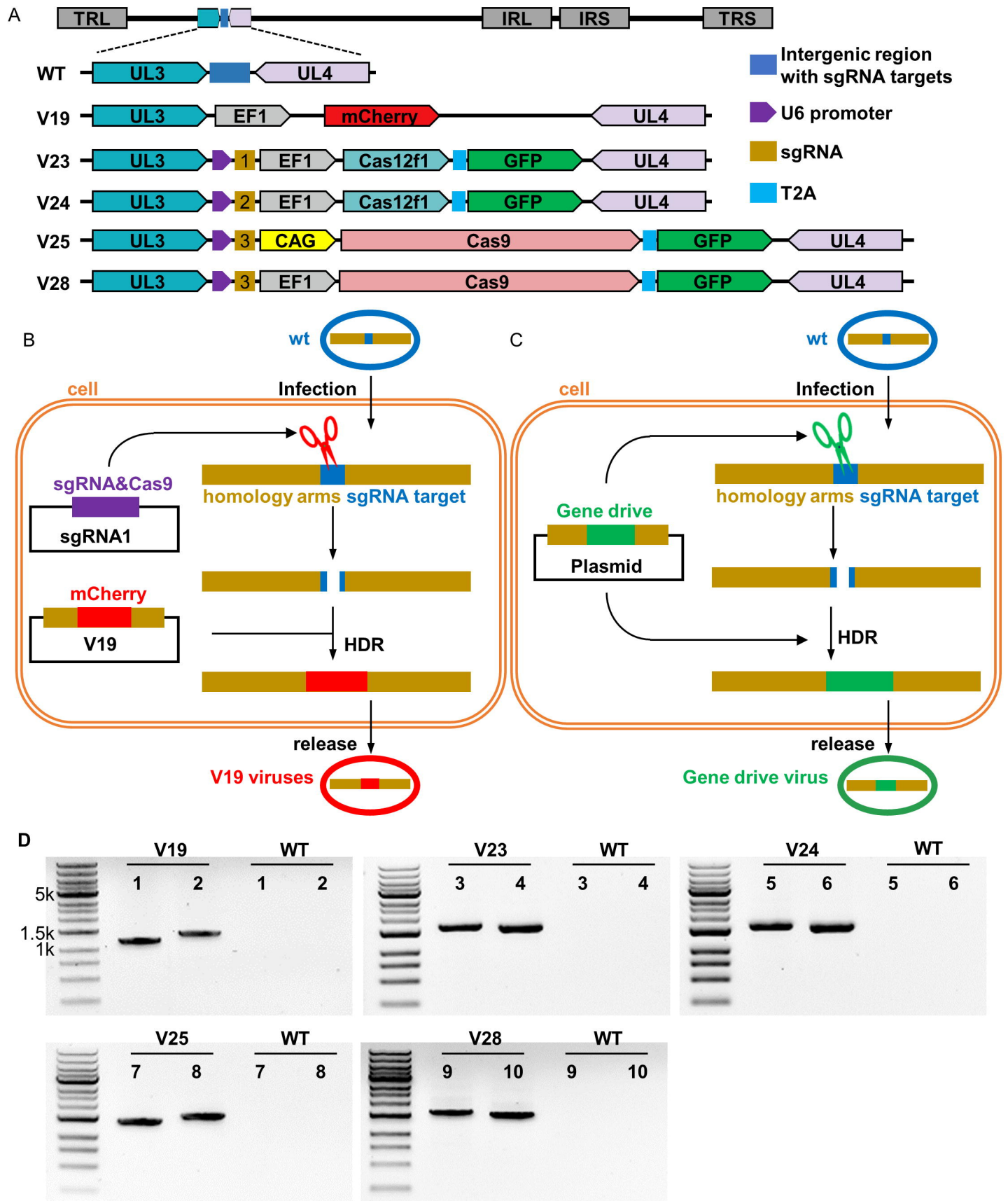
A
TRL
IRL
IRS
TRS
WT
UL3
UL4
V19
EF1
mCherry
V23
1
Cas12f1
GFP
V24
2
V25
3
CAG
Cas9
V28
Intergenic region with sgRNA targets
U6 promoter
sgRNA
T2A
B
wt
cell
Infection
sgRNA&Cas9
sgRNA1
homology arms
sgRNA target
mCherry
V19
HDR
release
V19 viruses
C
Gene drive
Plasmid
Gene drive virus
D
V19
WT
V23
V24
V25
V28
5k
1.5k
1k

Fig 3

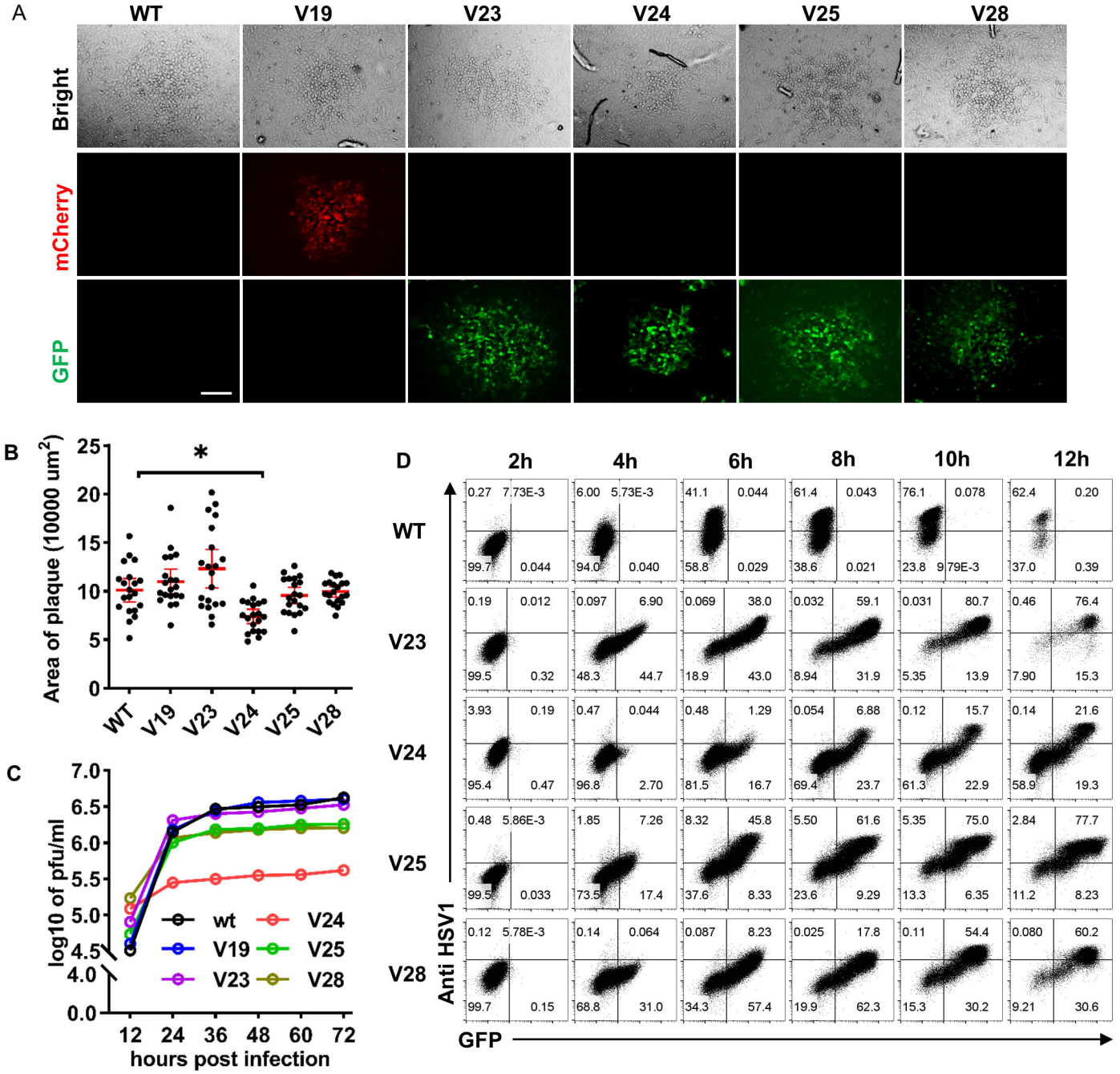
A
WT
V19
V23
V24
V25
V28
Bright
mCherry
GFP
B
Area of plaque (10000 um2)
*
WT
V19
V23
V24
V25
V28
C
log10 of pfu/ml
wt
V19
V23
V24
V25
V28
hours post infection
D
2h
4h
6h
8h
10h
12h
WT
V23
V24
V25
V28
Anti HSV1
GFP

Fig 4

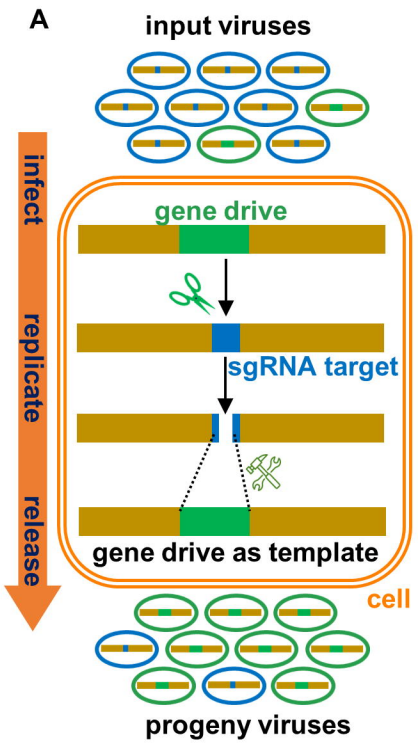
A
input viruses
infect
replicate
release
gene drive
sgRNA target
gene drive as template
cell
progeny viruses

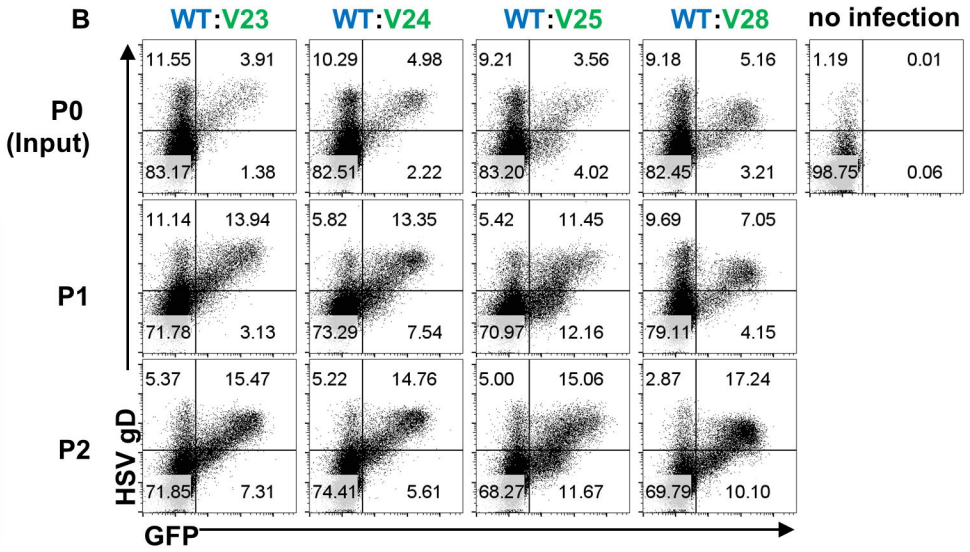
B
WT:V23
WT:V24
WT:V25
WT:V28
no infection
P0 (Input)
P1
P2
HSV gD
GFP
11.55 3.91 83.17 1.38
10.29 4.98 82.51 2.22
9.21 3.56 83.20 4.02
9.18 5.16 82.45 3.21
1.19 0.01 98.75 0.06
11.14 13.94 71.78 3.13
5.82 13.35 73.29 7.54
5.42 11.45 70.97 12.16
9.69 7.05 79.11 4.15
5.37 15.47 71.85 7.31
5.22 14.76 74.41 5.61
5.00 15.06 68.27 11.67
2.87 17.24 69.79 10.10

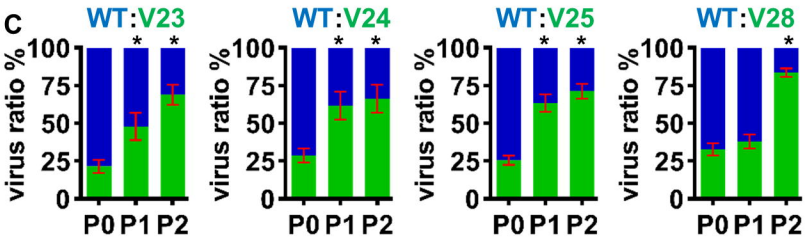
C
WT:V23
WT:V24
WT:V25
WT:V28
virus ratio %
100
75
50
25
0
P0 P1 P2

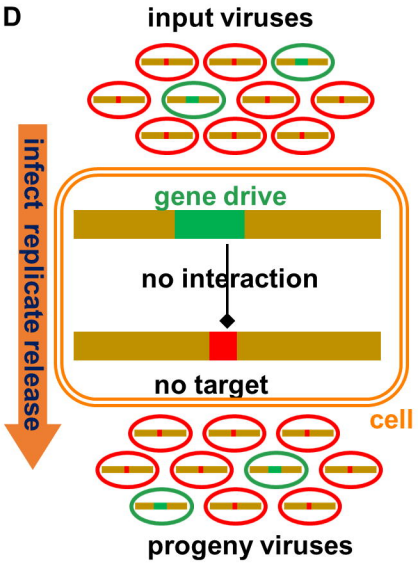
D
input viruses
infect
replicate
release
gene drive
no interaction
no target
cell
progeny viruses

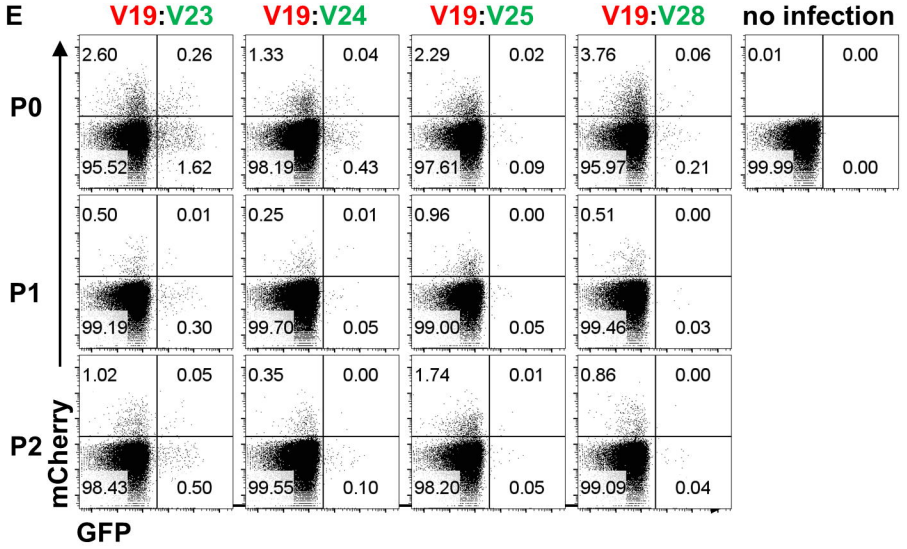
E
V19:V23
V19:V24
V19:V25
V19:V28
no infection
P0
P1
P2
mCherry
GFP
2.60 0.26 95.52 1.62
1.33 0.04 98.19 0.43
2.29 0.02 97.61 0.09
3.76 0.06 95.97 0.21
0.01 0.00 99.99 0.00
0.50 0.01 99.19 0.30
0.25 0.01 99.70 0.05
0.96 0.00 99.00 0.05
0.51 0.00 99.46 0.03
1.02 0.05 98.43 0.50
0.35 0.00 99.55 0.10
1.74 0.01 98.20 0.05
0.86 0.00 99.09 0.04

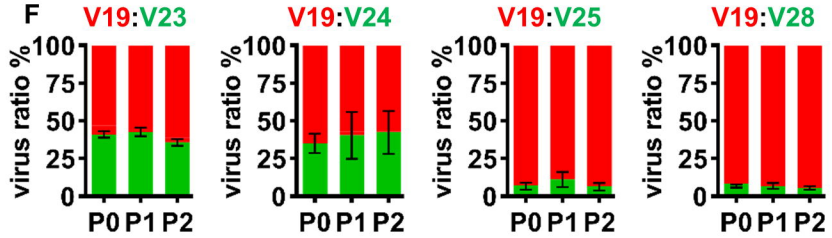
F
V19:V23
V19:V24
V19:V25
V19:V28
virus ratio %
100
75
50
25
0
P0 P1 P2

Fig 5

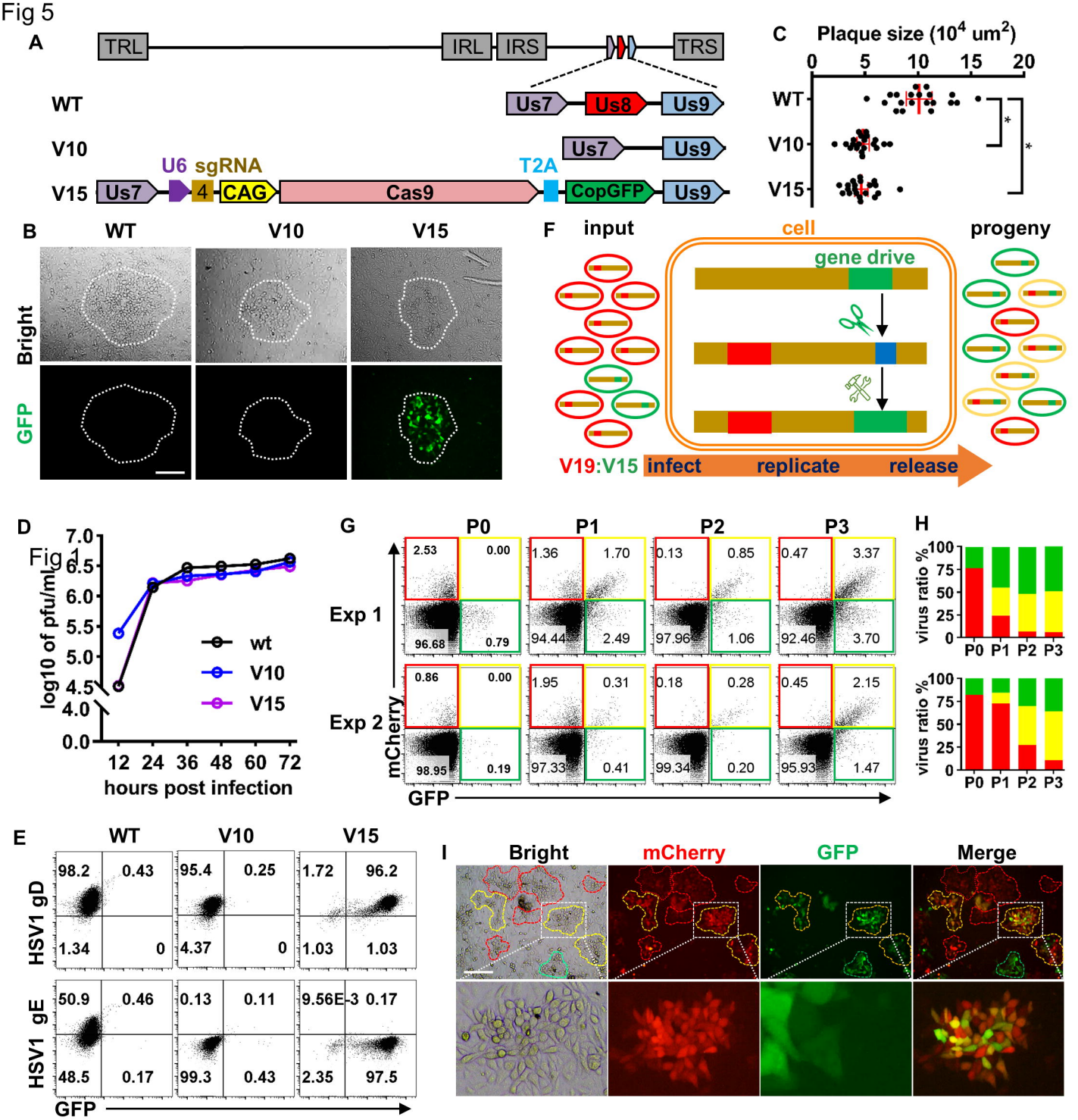
A
TRL
IRL
IRS
TRS
WT
Us7
Us8
Us9
V10
Us7
Us9
U6 sgRNA
T2A
V15
Us7
4
CAG
Cas9
CopGFP
Us9
C
Plaque size (10^4 um^2)
0
5
10
15
20
WT
V10
V15
*
*
B
WT
V10
V15
Bright
GFP
F
input
cell
progeny
gene drive
V19:V15
infect
replicate
release
D
Fig 1
log10 of pfu/mL
7.0
6.5
6.0
5.5
5.0
4.5
4.0
0.0
wt
V10
V15
12
24
36
48
60
72
hours post infection
G
P0
P1
P2
P3
Exp 1
Exp 2
mCherry
GFP
2.53
0.00
96.68
0.79
1.36
1.70
94.44
2.49
0.13
0.85
97.96
1.06
0.47
3.37
92.46
3.70
0.86
0.00
98.95
0.19
1.95
0.31
97.33
0.41
0.18
0.28
99.34
0.20
0.45
2.15
95.93
1.47
H
virus ratio %
100
75
50
25
0
P0
P1
P2
P3
E
WT
V10
V15
HSV1 gD
98.2
0.43
1.34
0
95.4
0.25
4.37
0
1.72
96.2
1.03
1.03
HSV1 gE
50.9
0.46
48.5
0.17
0.13
0.11
99.3
0.43
9.56E-3
0.17
2.35
97.5
GFP
I
Bright
mCherry
GFP
Merge

Fig 6

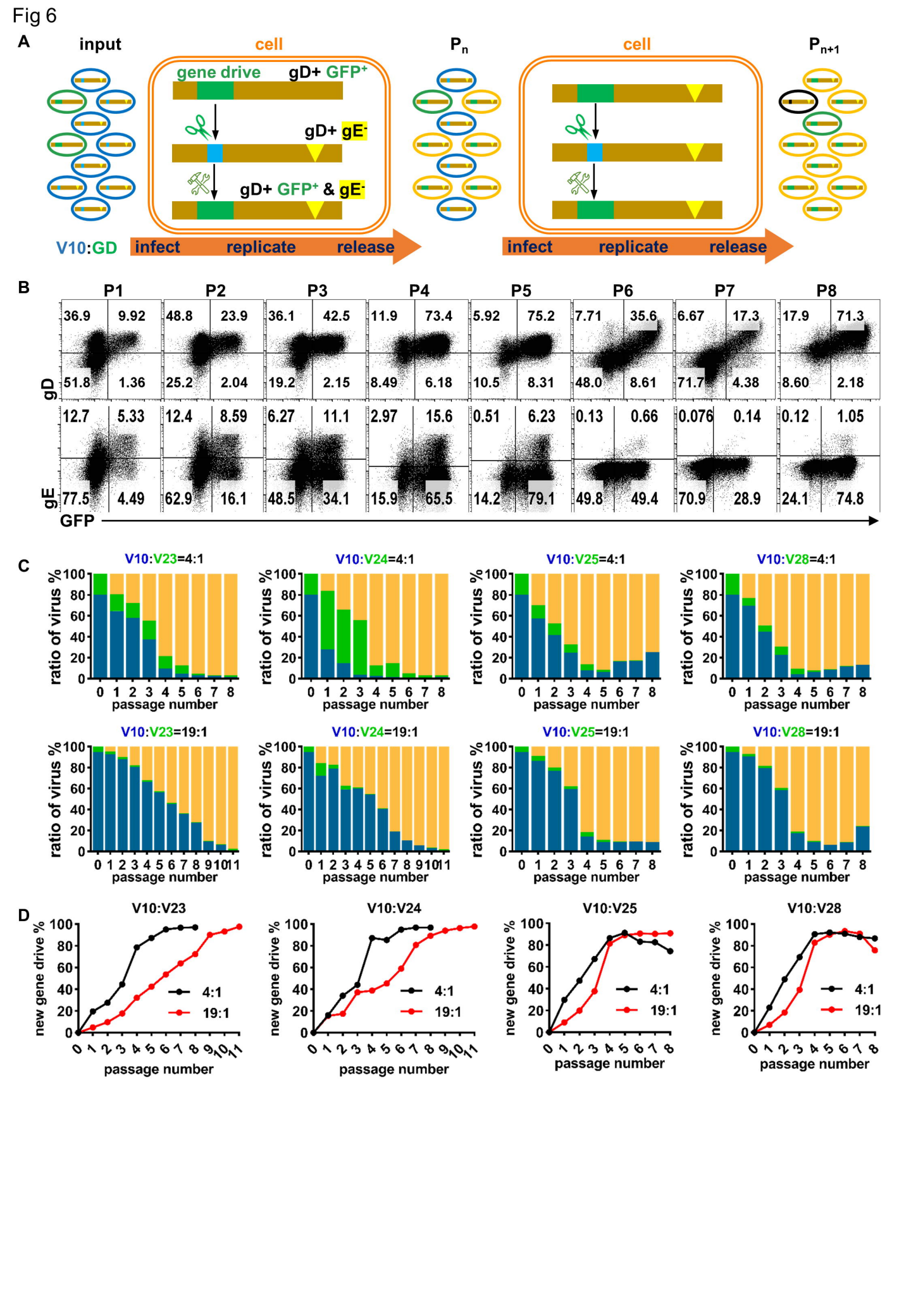
A
input
cell
gene drive
gD+ GFP+
gD+ gE-
gD+ GFP+ & gE-
Pn
cell
Pn+1
V10:GD
infect
replicate
release
infect
replicate
release
B
P1
P2
P3
P4
P5
P6
P7
P8
gD
gE
GFP
36.9 9.92 51.8 1.36
48.8 23.9 25.2 2.04
36.1 42.5 19.2 2.15
11.9 73.4 8.49 6.18
5.92 75.2 10.5 8.31
7.71 35.6 48.0 8.61
6.67 17.3 71.7 4.38
17.9 71.3 8.60 2.18
12.7 5.33 77.5 4.49
12.4 8.59 62.9 16.1
6.27 11.1 48.5 34.1
2.97 15.6 15.9 65.5
0.51 6.23 14.2 79.1
0.13 0.66 49.8 49.4
0.076 0.14 70.9 28.9
0.12 1.05 24.1 74.8
C
V10:V23=4:1
V10:V24=4:1
V10:V25=4:1
V10:V28=4:1
V10:V23=19:1
V10:V24=19:1
V10:V25=19:1
V10:V28=19:1
ratio of virus %
passage number
D
V10:V23
V10:V24
V10:V25
V10:V28
new gene drive %
4:1
19:1
passage number

Fig 7

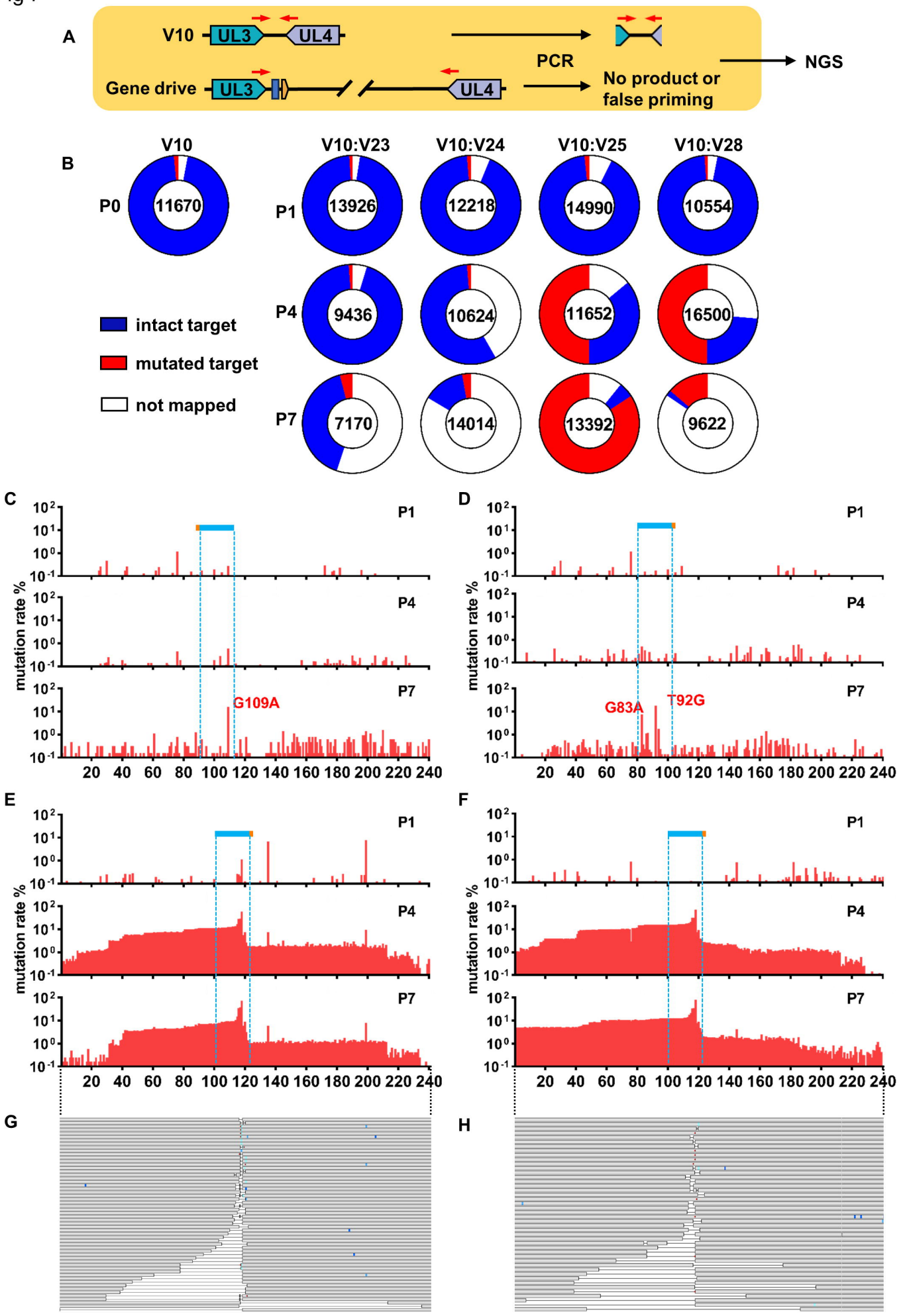
A
V10
UL3
UL4
Gene drive
PCR
No product or false priming
NGS
B
V10
V10:V23
V10:V24
V10:V25
V10:V28
P0
P1
P4
P7
11670
13926
12218
14990
10554
9436
10624
11652
16500
7170
14014
13392
9622
intact target
mutated target
not mapped
C
D
E
F
G
H
mutation rate %
G109A
G83A
T92G